

An optical clock with neutral atoms confined in a shallow trap

Pierre Lemonde¹ and Peter Wolf²¹ SYRTE, Observatoire de Paris
61, Avenue de l'observatoire, 75014, Paris, France² Bureau International des Poids et Mesures,
Pavillon de Breteuil,
92312 Sevres Cedex, France
(Dated: May 24, 2019)

We study the trap depth requirement for the realization of an optical clock using atoms confined in a lattice. We show that site-to-site tunnelling leads to a residual sensitivity to the atom dynamics hence requiring large depths (50 to 100 E_r for Sr) to avoid any frequency shift or line broadening of the atomic transition at the 10^{-17} – 10^{-18} level. Such large depths and the corresponding laser power may, however, lead to difficulties (e.g. higher order light shifts, two-photon ionization, technical difficulties) and therefore one would like to operate the clock in much shallower traps. To circumvent this problem we propose the use of an accelerated lattice. Acceleration lifts the degeneracy between adjacent potential wells which strongly inhibits tunnelling. We show that using the Earth's gravity, much shallower traps (down to 5 E_r for Sr) can be used for the same accuracy goal.

PACS numbers: 06.20.-f, 32.80.Qk, 42.50.Vk, 03.65.Xp

I. INTRODUCTION

The control of the external degrees of freedom of atoms, ions and molecules and of the associated frequency shifts and line broadenings is a long standing issue of the fields of spectroscopy and atomic frequency standards. They have been a strong motivation for the development of many widely spread techniques like the use of buffer gases [1], Ramsey spectroscopy [2], saturated spectroscopy [3], two-photon spectroscopy [4], trapping and laser cooling [5, 6], etc.

In the case of ions, the problem is now essentially solved since they can be trapped in relatively low fields and cooled to the zero point of motion of such traps [5]. In this state, the ions are well within the Lamb-Dicke regime [1] and experience no recoil nor first order Doppler effect [5]. The fractional accuracy of today's best ion clocks lies in the range from 3 to 10^{-15} [7, 8, 9, 10, 11] with still room for improvement. The main drawback of trapped ion frequency standards is that only one to a few ions can contribute to the signal due to Coulomb repulsion. This fundamentally limits the frequency stability of these systems and puts stringent constraints on the frequency noise of the oscillator which probes the ions [12].

These constraints are relaxed when using a large number of neutral atoms [13] for which, however, trapping requires much higher fields, leading to shifts of the atomic levels. This fact has for a long time prevented the use of trapped atoms for the realization of atomic clocks and today's most accurate standards use freely falling atoms. Microwave fountains now have an accuracy slightly below 10^{-15} and are coming close to their foreseen ultimate

limit which lies around 10^{-16} [14], which is essentially not related to effects due to the atomic dynamics [15, 16]. In the optical domain, atomic motion is a problem and even with the use of ultra-cold atoms probed in a Ramsey-Borde interferometer [17], optical clocks with neutrals still suffer from the first order Doppler and recoil effects [18, 19, 20, 21]. Their state-of-the-art accuracy is about 10^{-14} [20].

The situation has recently changed with the proposal of the optical lattice clock [22]. The idea is to engineer a lattice of optical traps in such a way that the dipole potential is exactly identical for both states of the clock transition, independently of the dipole laser power and polarisation. This is achieved by tuning the trap laser to the so-called "magic wavelength" and by the choice of clock levels with zero electronic angular momentum. The original scheme was proposed for ^{87}Sr atoms using the strongly forbidden 1S_0 – 3P_0 line at 698 nm as a clock transition [23]. In principle however, it also works for all atoms with a similar level structure like Mg, Ca, Yb, Hg, etc. including their bosonic isotopes if one uses multi-photon excitation of the clock transition [24, 25].

In this paper we study the effect of the atom dynamics in the lattice on the clock performances. In ref. [22], it is implicitly assumed that each microtrap can be treated separately as a quadratic potential in which case the situation is very similar to the trapped ion case and then fully understood [5]. With an accuracy goal in the 10^{-17} – 10^{-18} range in mHz (corresponding to the mHz level in the optical domain), we shall see later on, that this is correct at very high trap depths only. The natural energy unit for the trap dynamics is the recoil energy associated with the absorption or emission of a photon of the lattice laser, $E_r = \frac{\hbar^2 k_L^2}{2m_a}$ with k_L the wave vector of the lattice laser and m_a the atomic mass. For Sr and for the above accuracy goal the trap depth U_0

Electronic address: pierre.lemonde@obspm.fr

corresponding to the independent trap limit it is typically $U_0 = 100 E_r$, which corresponds to a peak laser intensity of 25 kW / cm^2 .

For a number of reasons however, one would like to work with traps as shallow as possible. First, the residual shift by the trapping light of the clock transition is smaller and smaller at a decreasing trap depth. The first order perturbation is intrinsically cancelled by tuning to the magic wavelength except for a small eventual tensorial effect which depends on the hyperfine structure of the atom under consideration. Higher order terms may be much more problematic depending on possible coincidences between two-photon resonances and the magic wavelength [22, 26]. The associated shift scales as U_0^2 [47]. The shifts would then be minimized by a reduction of U_0 and its evaluation would be greatly improved if one can vary this parameter over a broader range. Second, for some of the possible candidate atoms, such as Hg for which the magic wavelength is about 340 nm , two-photon ionization can occur which may limit the achievable resonance width and lead to a frequency shift. Finally, technical aspects like the required laser power at the magic wavelength can be greatly relaxed if one can use shallow traps. This can make the experiment feasible or not if the magic wavelength is in a region of the spectrum where no readily available high power laser exists, such as in the case of Hg. For this atom, a trap depth of $100 E_r$ would necessitate a peak intensity of 500 kW / cm^2 at 340 nm .

When considering shallow traps, the independent trap limit no longer holds, and one cannot neglect tunnelling of the atoms from one site of the lattice to another. This leads to a delocalization of the atoms and to a band structure in their energy spectrum and associated dynamics. In section III we investigate the ultimate performance of the clock taking this effect into account. We show that depending on the initial state of the atoms in the lattice, one faces a broadening and/or a shift of the atomic transition of the order of the width of the lowest energy band of the system. For Sr, this requires U_0 of the order of $100 E_r$ to ensure a fractional accuracy better than 10^{-17} .

The deep reason for such a large required value of U_0 is that site-to-site tunnelling is a resonant process in a lattice. We show in section IV that a much lower U_0 can be used provided the tunnelling process is made non-resonant by lifting the degeneracy between adjacent sites. This can be done by adding a constant acceleration to the lattice, leading to the well-known Wannier-Stark ladder of states [27, 28]. More specially, we study the case where this acceleration is simply the Earth's gravity. The experimental realization of the scheme in this case is then extremely simple: the atoms have to be probed with a laser beam which propagates vertically. In this configuration, trap depths down to $U_0 \approx 5 E_r$ can be sufficient for the above accuracy goal.

II. CONFINED ATOMS COUPLED TO A LIGHT FIELD

In this section we describe the theoretical frame used to investigate the residual effects of the motion of atoms in an external potential. The internal atomic structure is approximated by a two-level system $|j_i\rangle$ and $|j_e\rangle$ with energy difference $\sim \hbar \omega_{eg}$. The internal Hamiltonian is:

$$\hat{H}_i = \hbar \omega_{eg} |j_e\rangle\langle j_i| \quad (1)$$

We introduce the coupling between $|j_i\rangle$ and $|j_e\rangle$ by a laser of frequency ω and wavevector \mathbf{k}_s propagating along the x direction:

$$\hat{H}_s = \hbar \cos(\omega t - \mathbf{k}_s \mathbf{x}) |j_e\rangle\langle j_i| + \text{h.c.} \quad (2)$$

with the Rabi frequency.

In the following we consider external potentials induced by trap lasers tuned at the magic wavelength and/or by gravity. The external potential \hat{H}_{ext} is then identical for both $|j_i\rangle$ and $|j_e\rangle$ with eigenstates $|j_n\rangle$ obeying $\hat{H}_{\text{ext}} |j_n\rangle = \hbar \epsilon_n |j_n\rangle$ (Note that $|j_n\rangle$ can be a continuous variable in which case the discrete sums in the following are replaced by integrals). If we restrict ourselves to experiments much shorter than the lifetime of state $|j_i\rangle$ (for ^{87}Sr , the lifetime of the lowest 3P_0 state is 100 s) spontaneous emission can be neglected and the evolution of the general atomic state

$$|j_{\text{at}}\rangle = \sum_m a_m^g e^{i \epsilon_m t} |j_n\rangle\langle j_i| + a_m^e e^{i(\epsilon_{eg} + \epsilon_m)t} |j_n\rangle\langle j_e| \quad (3)$$

is driven by

$$i \hbar \frac{\partial}{\partial t} |j_{\text{at}}\rangle = (\hat{H}_{\text{ext}} + \hat{H}_i + \hat{H}_s) |j_{\text{at}}\rangle \quad (4)$$

leading to the following set of coupled equations

$$\begin{aligned} i \hbar \frac{\partial}{\partial t} a_m^g &= \sum_{m^0} \frac{1}{2} e^{i \epsilon_{m^0} t} \langle j_n | \hat{H}_s | j_n^0 \rangle a_{m^0}^e \\ i \hbar \frac{\partial}{\partial t} a_m^e &= \sum_{m^0} \frac{1}{2} e^{i \epsilon_{m^0} t} \langle j_n | \hat{H}_s | j_n^0 \rangle a_{m^0}^g \end{aligned} \quad (5)$$

To derive eq. (5) we have made the usual rotating wave approximation (assuming $\omega - \omega_{eg} \ll \omega_{eg}$) and defined $\epsilon_{m^0} = \epsilon_{eg} + \epsilon_m - \epsilon_{m^0}$.

In the case of free atoms, $\hat{H}_{\text{ext}} = \frac{\hbar^2 \mathbf{k}_a^2}{2m_a}$ with \mathbf{k}_a the atomic momentum and m_a the atomic mass. The eigenstates are then plane waves: $|j_i\rangle \sim e^{i \mathbf{k}_i \mathbf{x}}$ is coupled to $|j_e\rangle \sim e^{i \mathbf{k}_e \mathbf{x}}$ with $\mathbf{k}_e = \mathbf{k}_i + \mathbf{k}_s$. One recovers the first order Doppler and recoil frequency shifts.

Conversely in a tightly confining trap $\langle j_n | \hat{H}_s | j_n^0 \rangle \ll \langle j_n | \hat{H}_s | j_n^i \rangle$, and the spectrum of the system consists of a set of unshifted resonances corresponding to each state of the external Hamiltonian. Motional effects then reduce to the line pulling of these resonances by small (detuned) sidebands [5].

III. PERIODIC POTENTIAL

A. Eigenstates and coupling by the probe laser

We now consider the case of atoms trapped in an optical lattice. As is clear from eq. (5), only the motion of the atoms along the probe laser propagation axis plays a role in the problem and we restrict the analysis to 1D [48]. We assume that the lattice is formed by a standing wave leading to the following external hamiltonian:

$$\hat{H}_{\text{ext}}^I = \frac{\hbar^2 k_1^2}{2m_a} + \frac{U_0}{2} (1 - \cos(2k_1 \hat{x})); \quad (6)$$

where k_1 is the wave vector of the trap laser. The eigenstates $|n; q\rangle$ and eigenenergies $\epsilon_{n,q}^I$ of \hat{H}_{ext}^I are derived from the Bloch theorem [29]. They are labelled by two quantum numbers: the band index n and the quasi-momentum q . Furthermore they are periodic functions of q with period $2k_1$ and the usual convention is to restrict oneself to the first Brillouin zone $q \in [-k_1, k_1]$.

Following a procedure given in Ref. [28] a numerical solution to this eigenvalue problem can be easily found in the momentum representation. The atomic plane wave with wave vector \mathbf{k} obeys

$$\hat{H}_{\text{ext}}^I |j\rangle = \left(\frac{\hbar^2 k^2}{2m_a} + \frac{U_0}{2} \right) |j\rangle = \frac{U_0}{4} (j + 2k_1 i + j - 2k_1 i); \quad (7)$$

For each value of q , the problem then reduces to the diagonalization of a real tridiagonal matrix giving the eigenenergies and eigenvectors as a linear superposition of plane waves:

$$\begin{aligned} \hat{H}_{\text{ext}}^I |n; q\rangle &= \sum_{i=-1}^1 \epsilon_{n,q+i}^I |n; q+i\rangle \\ |n; q\rangle &= \sum_{i=-1}^1 C_{n,i;q} |i; q\rangle; \end{aligned} \quad (8)$$

with $i; q = q + 2ik_1$. For each value of q one obtains a discrete set of energies $\epsilon_{n,q}^I$ and coefficients $C_{n,i;q}$, which are real and normalized such that $\sum_i C_{n,i;q}^2 = 1$. In figures 1 and 2 are shown $\epsilon_{n,q}^I$ and $C_{0,i;q}$ for various values of U_0 . Except when explicitly stated, all numerical values throughout the paper are given for ^{87}Sr at a lattice laser wavelength 813 nm which corresponds to the magic wavelength reported in Ref. [30]. In frequency units E_r then corresponds to 3.58 kHz. In figure 3 is shown the width $(\epsilon_{n,q=k_1}^I - \epsilon_{n,q=0}^I)$ of the lowest energy bands as a function of U_0 in units of E_r and in frequency units.

Substituting $\sum_i C_{n,i;q} |i; q\rangle$ and $\sum_i C_{n^0,i;q^0} |i; q^0\rangle$ in eq. (5), the action of the probe laser is described by the coupled equations

$$\begin{aligned} i\dot{a}_{n,q}^g &= \sum_{n^0} \frac{C_{n^0,0;q^0}}{2} e^{i \frac{n^0 - n}{q} t} a_{n^0,q^0+k_s}^e \\ i\dot{a}_{n,q+k_s}^e &= \sum_{n^0} \frac{C_{n^0,0;q^0}}{2} e^{-i \frac{n^0 - n}{q} t} a_{n^0,q}^g; \end{aligned} \quad (9)$$

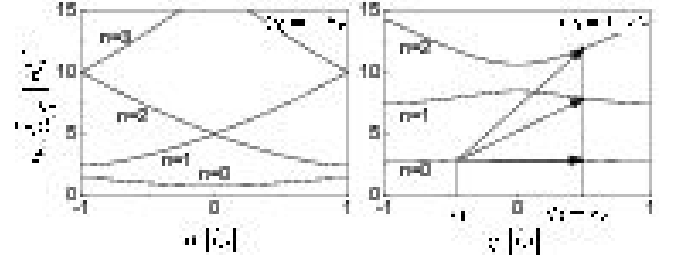


FIG. 1: Band structure for two different lattice depth: $U_0 = 2 E_r$ (left) and $U_0 = 10 E_r$ (right). Each state $|n; q\rangle$ is coupled to all the states $|n^0; q^0 + k_s\rangle$ by the probe laser.

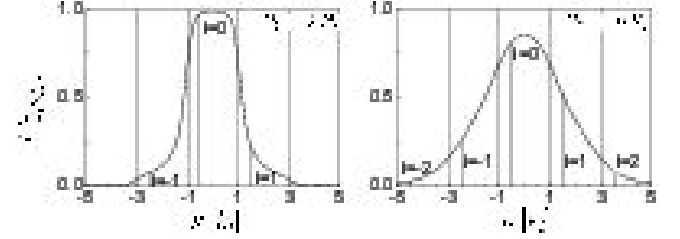


FIG. 2: $C_{0,i;q}$ for two different lattice depth: $U_0 = 2 E_r$ (left) and $U_0 = 10 E_r$ (right). The bold vertical lines illustrate the case $q = \pm k_1$. The dotted lines delimit the Brillouin zones. For a state $|n=0; q=ak_1\rangle$ with a 2π shift the solid envelope gives the contribution of the plane waves $|i; q+ak_1\rangle = |i; q+2ik_1\rangle$.

with $\sum_{n^0} C_{n^0,0;q^0} = 1$ and $\sum_{n^0} C_{n^0,0;q^0}^2 = 1$. As expected from the structure of the Bloch vectors in (8), the translation in momentum space $e^{ik_s \hat{x}}$ due to the probe laser leads to the coupling of a given state $|n; q\rangle$ to the whole set $|n^0; q+k_s\rangle$ (see figure 1) with a coupling strength $C_{n^0,0;q^0}$ and a shift with respect to the atomic resonance $\epsilon_{n^0,q^0+k_s}^I - \epsilon_{n,q}^I$. Both quantities depend on n, n^0 and q and to go further we have to make assumptions on the initial state of the atoms in the lattice.

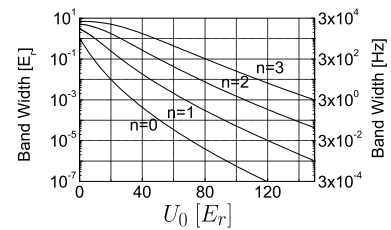


FIG. 3: Lowest four band widths as a function of the lattice depth U_0 in units of E_r (left scale) and in frequency units (right scale).

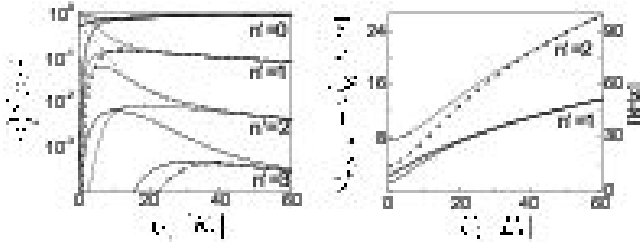


FIG. 4: Left: Relative strength of the transitions to different bands ($n = 0 \dots n^0$) for an atom prepared in state $j = 0; q = k_1 i$ (bold lines), $j = 0; q = k_1 = 2i$ and $j = 0; q = k_1 = 2i$ (thin lines). Right: detuning of the first two sidebands for an atom prepared in state $j = 0; q = k_1 i$ (bold lines) and $j = 0; q = 0i$ (thin lines) in units of E_r (left scale) and in frequency units (right scale).

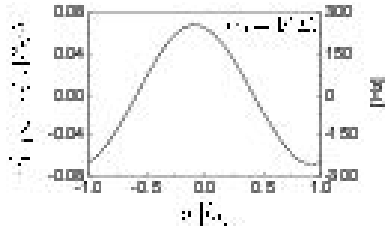


FIG. 5: Shift of the "carrier" resonance in the first band for a lattice depth $U_0 = 10 E_r$. Left scale: in units of E_r . Right scale: in frequency units.

B. Discussion

We first consider the case where the initial state is a pure $j; q_i$ state. The strengths of the resonances $n; n^0_q$ are shown in figure 4 for the case $n = 0$ and various values of q . At a growing lattice depth $n; n^0_q$ become independent of q and the strength of all "sidebands" ($n^0 \neq 0$) asymptotically decreases as $U_0^{-j^0 - n^0 + 4}$ for the benefit of the "carrier" ($n^0 = n$). The frequency separation of the resonances rapidly increases with U_0 (Fig. 4). For U_0 as low as $5 E_r$, this separation is of the order of 10 kHz. For narrow resonances (which are required for an accurate clock) they can be treated separately and the effect of the sidebands on the carrier is negligible. If for example one reaches a carrier width of 10 Hz, the sideband pulling is of the order of 10^{-5} Hz. On the other hand, the "carrier" frequency is shifted from the atomic frequency by $\Delta_{n; q+k_s}^I - \Delta_{n; q}^I$ due to the band structure. This shift is of the order of the width of the n^{th} band (Fig. 5 and 3). It can be seen as a residual Doppler and recoil effect for atoms trapped in a lattice and is a consequence of the complete delocalisation of the eigenstates of the system over the lattice. The "carrier" shift is plotted in figure 5 for the case $n = 0$ and $U_0 = 10 E_r$. For this shift to be as small as 5 mHz over the whole lowest band, which corresponds in fractional units to 10^{-17} for Sr atoms probed on the $^1S_0 \rightarrow ^3P_0$ transition, the lattice depth should be at least $90 E_r$ (Fig. 3).

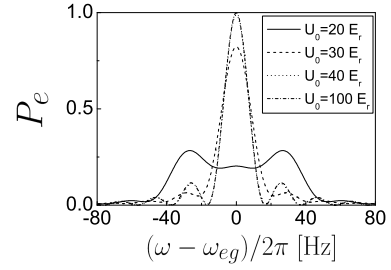


FIG. 6: Expected resonances in the case where the first band is uniformly populated for $\Omega = 10$ Hz and $U_0 = 20 E_r; 30 E_r; 40 E_r$; and $100 E_r$. The duration of the interaction is such that the transition probability at resonance is maximized.

Another extreme situation is the case where one band is uniformly populated. In this case the "carrier" shift averaged over q cancels and one can hope to operate the clock at a much lower U_0 than in the previous case. The problem is then the ultimate linewidth that can be achieved in the system, which is of the order of the width of the band and is reminiscent of Doppler broadening. This is illustrated in figure 6 for which we have computed the expected "carrier" resonances in the case where the lowest band is uniformly populated, by numerically solving equations (5). This was done for a Rabi frequency $\Omega = 10$ Hz and an interaction duration which is adjusted for each trapping depth so as to maximize the transition probability at zero detuning. We have checked that all resonances plotted in figure 6 are not shifted to within the numerical accuracy (less than 10^{-5} Hz). However, at decreasing U_0 the contrast of the resonance starts to drop for $U_0 < 40 E_r$ and the resonance broadens progressively, becoming unusable for precise spectroscopy when the width of the energy band reaches the Rabi frequency. To get more physical insight into this phenomenon, let's consider the particular example of this uniform band population where one well of the lattice is initially populated. This corresponds to a given relative phase of the Bloch states such that the interference of the Bloch vectors is destructive everywhere except in one well of the lattice. The time scale for the evolution of this relative phase is the inverse of the width of the populated energy band which then corresponds to the tunnelling time towards delocalization (once the relative phases have evolved significantly, the destructive/constructive interferences of the initial state no longer hold). The broadening and loss of contrast shown in figure 6 can be seen as the Doppler effect associated with this tunnelling motion.

The two cases discussed above (pure $j; q_i$ state and uniform superposition of all states inside a band: $dq; j; q_i$) correspond to the two extremes one can obtain when populating only the bottom band. They illustrate the dilemma one has to face: either the resonance is affected by a frequency shift of the order of the width of the bottom band (pure state), or by a broadening of the same order (superposition state), or by a combina-

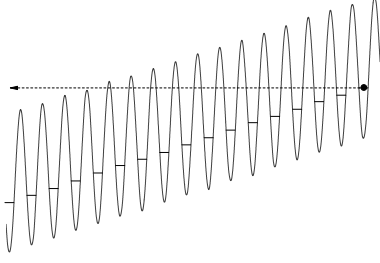


FIG. 7: External potential seen by the atoms in the case of a vertical lattice ($U_0 = 5E_r$). An atom initially trapped in one well of the lattice will end up in the continuum by tunnel effect. For $U_0 = 5E_r$ the lifetime of the quasi-bound state of each well is about 10^{10} s.

tion of both (general case). In either case the solution is to increase the trap depth in order to decrease the energy width of the bottom band.

In the experimental setup described in [30] about 90 % of the atoms are in the lowest band and can be selected by an adequate sequence of laser pulses. The residual population of excited bands can then be made negligible ($< 10^{-3}$). On the other hand, knowing and controlling with accuracy the population of the various j i states in the ground band is a difficult task. The actual initial distribution of atomic states will lie somewhere between a pure state in the bottom band and a uniform superposition of all states in the bottom band. If we assume that the population of the j i states in the ground band can be controlled so that the frequency shift averages to within one tenth of the band width, then a fractional accuracy goal of 10^{-17} implies $U_0 = 70E_r$ or more. Note that due to the exponential dependence of the width of the ground band on U_0 (see figure 3) the required lattice depth is largely insensitive to an improvement in the control of the initial state. If for example the averaging effect is improved down to 1 % the depth requirement drops from $70E_r$ to $50E_r$. Consequently, operation of an optical lattice clock requires relatively deep wells and correspondingly high laser power, which, in turn, is likely to lead to other difficulties as described in the introduction.

Fortunately, the requirement of deep wells can be significantly relaxed by adding a constant acceleration to the lattice, as described in the next section.

IV. PERIODIC POTENTIAL IN AN ACCELERATED FRAME

A. Wannier-Stark states and coupling by the probe laser

The shift and broadening encountered in the previous section are both due to site-to-site tunnelling and to the corresponding complete delocalization of the eigenstates

of the lattice. As is well-known from solid-state physics, one way to localize the atoms is to add a linear component to the Hamiltonian [27]: adjacent wells are then shifted in energy, which strongly inhibits tunnelling. In this section we study the case where the lattice and probe laser are oriented vertically so that gravity plays the role of this linear component. The external Hamiltonian is then:

$$\hat{H}_{\text{ext}}^{\text{II}} = \frac{\hbar^2 k_1^2}{2m_a} + \frac{U_0}{2} (1 - \cos(2k_1 \hat{x})) + m_a g \hat{x}; \quad (10)$$

with g the acceleration of the Earth's gravity. This Hamiltonian supports no true bound states, as an atom initially confined in one well of the lattice will end up in the continuum due to tunnelling under the influence of gravity (Fig. 7). This effect is known as Landau-Zener tunnelling and can be seen as non-adiabatic transitions between bands induced by the linear potential in the Bloch representation [31, 32, 33, 34]. The timescale for this effect however increases exponentially with the depth of the lattice and for the cases considered here is orders of magnitude longer than the duration of the experiment [49]. In the case of Sr in an optical lattice, and for U_0 as low as $5E_r$, the lifetime of the ground state of each well is about 10^{10} s! The coupling due to gravity between the ground and excited bands can therefore be neglected here. In the frame of this approximation the problem of finding the "eigenstates" of $\hat{H}_{\text{ext}}^{\text{II}}$ reduces to its diagonalization in a sub-space restricted to the ground band [35, 36] (we drop the band index in the following to keep notations as simple as possible). We are looking for solutions to the eigenvalue equation, of the form :

$$\begin{aligned} \hat{H}_{\text{ext}}^{\text{II}} \tilde{\Psi}_m &= \tilde{\epsilon}_m^{\text{II}} \tilde{\Psi}_m \\ \tilde{\Psi}_m &= \int_{k_1} dq b_m(q) \tilde{\Psi}_i \end{aligned} \quad (11)$$

In eq. (11) the $\tilde{\Psi}_i$ are the Bloch eigenstates of $\hat{H}_{\text{ext}}^{\text{I}}$ (c.f. section III) for the bottom energy band ($n = 0$), m is a new quantum number, and the $b_m(q)$ are periodic: $b_m(q + 2\pi k_1) = b_m(q)$. After some algebra, eq. (11) reduce to the differential equation

$$(\tilde{\epsilon}_q^{\text{I}} - \tilde{\epsilon}_m^{\text{II}}) b_m(q) + i m_a g \partial_q b_m(q) = 0 \quad (12)$$

where $\tilde{\epsilon}_q^{\text{I}}$ is the eigenvalue of the Bloch state $j = 0; q$ of section III. Note that equations (11) and (12) only hold in the limit where Landau-Zener tunnelling between energy bands is negligible. Otherwise, terms characterising the contribution of the other bands must be added and the description of the quasi-bound states is more complex [28, 37]. In our case the periodicity of $b_m(q)$ and a normalization condition lead to a simple solution of the form

$$\begin{aligned} \tilde{\epsilon}_m^{\text{II}} &= \tilde{\epsilon}_0^{\text{II}} + m_a g \\ b_m(q) &= \frac{1}{2\pi k_1} e^{-\frac{i}{m_a g} (q - \tilde{\epsilon}_m^{\text{II}})} \end{aligned} \quad (13)$$

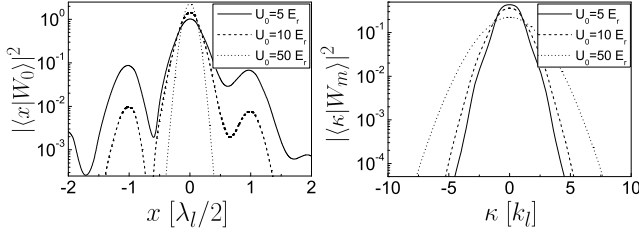


FIG. 8: Wannier-Stark states in position (left) and momentum (right) representation for $U_0 = 5 E_r$, $U_0 = 10 E_r$ and $U_0 = 50 E_r$. Numerically we first compute the momentum representation $\langle \kappa | W_m \rangle = b_m(\kappa) C_0$, and then obtain the position representation by Fourier transformation.

with the definitions $\langle 0 | = \frac{1}{2k_1} \int_{-\infty}^{\infty} dq \langle 0 |$, $\sim_g = m_a g_1 = 2$, and $\langle 0 | = \langle 0 |$ with $0 = 0$. The $|W_m\rangle$ states are usually called Wannier-Stark states and their wave functions are plotted in figure 8 for various trap depths. In the position representation $|W_m\rangle$ exhibits a main peak in the m^{th} well of the lattice and small revivals in adjacent wells. These revivals decrease exponentially at increasing lattice depth. At $U_0 = 10 E_r$ the first revival is already a hundred times smaller than the main peak. Conversely, in the momentum representation, the distribution gets broader with increasing U_0 . The phase shift between b_m and b_{m-1} in (13), $b_m(q) = e^{i q = k_1} b_{m-1}(q)$, corresponds to a translational symmetry of the Wannier-Stark states in the position representation $\langle x + 1 = 2 \rangle |W_m\rangle = \langle x | W_{m-1}\rangle$. The discrete quantum number m is the "well index" characterising the well containing the main peak of the wave function $\langle x | W_m\rangle$, and, as intuitively expected, the energy separation between adjacent states is simply the change in gravitational potential between adjacent wells: $\sim_g = m_a g_1 = 2$.

Substituting $\langle m | \langle W_m |$ and $|W_m\rangle$ in eq. (5) shows that the effect of the probe laser is to couple the Wannier-Stark states to their neighbours by the translation in momentum space $e^{ik_s x}$, with the coupling strengths

$$\langle W_m | e^{ik_s x} | W_{m-1} \rangle = \int_{-\infty}^{\infty} d b_m(\kappa + k_s) b_{m-1}(\kappa) C_0; C_0; \kappa + k_s; \quad (14)$$

obtained from direct substitution of (11) and (8) [50].

Using the translational symmetry of the Wannier-Stark states it is easy to show that

$$\langle W_m | e^{ik_s x} | W_{m-1} \rangle = e^{i m k_s = k_1} \langle W_0 | e^{ik_s x} | W_{m-1} \rangle; \quad (15)$$

From that property, equation (14), and using $b_m(\kappa) = b_m(\kappa)$ (note that $q = \kappa$) one can then show that

$$\langle W_m | e^{ik_s x} | W_{m+j} \rangle = e^{i j k_s = k_1} \langle W_m | e^{ik_s x} | W_{m-j} \rangle; \quad (16)$$

which is a useful result when studying the symmetry of coupling to neighbouring states (see next section).

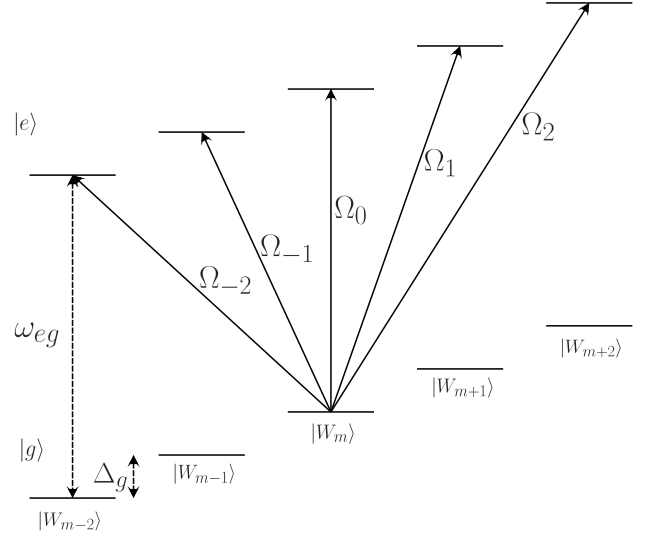


FIG. 9: Wannier-Stark ladder of states and coupling between states by the probe laser.

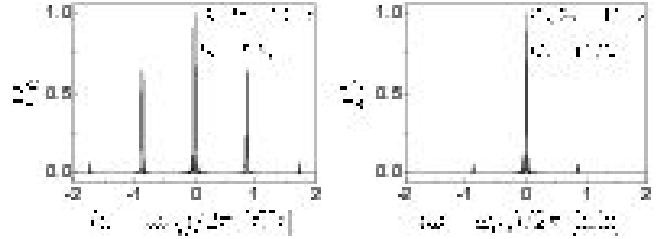


FIG. 10: Computed resonances when the initial state is a pure Wannier-Stark state. Left: $U_0 = 5 E_r$, right: $U_0 = 10 E_r$. Both resonances are plotted for an effective Rabi frequency of the carrier $\frac{\Omega}{2} = 10 \text{ Hz}$ and for an interaction time of 50 ms.

The differential equations (5), governing the evolution of the different states under coupling to the probe laser are then

$$\begin{aligned} i \dot{a}_m^g &= \sum_{m=0}^{\infty} \frac{m-m_0}{2} e^{i m_0 \frac{k_s}{k_1}} e^{i m-m_0 t} a_{m_0}^e \quad (17) \\ i \dot{a}_m^e &= \sum_{m=0}^{\infty} \frac{m_0-m}{2} e^{i m \frac{k_s}{k_1}} e^{i m_0-m t} a_{m_0}^g; \end{aligned}$$

in which we have used (15) and defined $a_m = \langle W_0 | e^{ik_s x} | W_m \rangle$ and $a_m = \langle W_{m_0} | e^{ik_s x} | W_m \rangle$.

B. Discussion

We now study the case where the initial state of the atom is a pure Wannier-Stark state. According to eq. (17) excitation by the laser will lead to a set of resonances separated by \sim_g (see Fig. 9). In the case of Sr, $\sim_g = 866 \text{ Hz}$ and for the narrow resonances required for high performance clock operation, they are easily resolved. The resonances obtained by first numerically in-

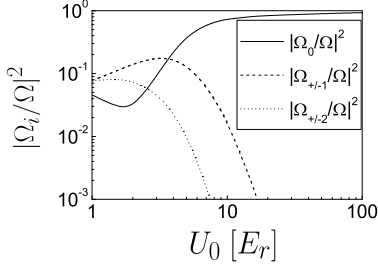


FIG. 11: Relative strength of the carrier $j_0 = j^2$ and of the first four sidebands $j_{\pm 1} = j^2$ and $j_{\pm 2} = j^2$ as a function of the lattice depth U_0 .

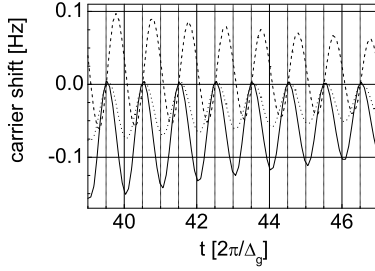


FIG. 12: Frequency shift of the carrier as a function of the interaction duration in the case where the initial state of the atom is a coherent superposition of neighbouring Wannier-Stark states. Solid line: $a_n^g(t=0) = a_{n+1}^g(t=0)$ for all n . Dashed line: $a_n^g(t=0) = a_{n+1}^g(t=0)e^{i\pi/2}$ for all n . Dotted line: $a_{-1}^g(t=0) = a_0^g(t=0)$ and $a_n^g(t=0) = 0$ for $n \neq -1; 0$. The shift is defined as the equilibrium point of a frequency servo loop using a square frequency modulation of optimal depth and computed for $U_0 = 5E_r$ and a carrier Rabi frequency $\Omega_0/2 = 10\text{ Hz}$. The interaction duration corresponding to a π pulse is $t_g/2 = 43.3$.

Integrating (14) and then numerically solving (17) are plotted in figure 10 for the cases $U_0 = 5E_r$ and $U_0 = 10E_r$. They exhibit remarkable properties. First the "carrier" (which corresponds to the transition $|W_{m+1}\rangle \leftrightarrow |W_m\rangle$) has a frequency which exactly matches the atomic frequency ω_{eg} . It also doesn't suffer from any broadening or contrast limitation (provided the side bands are resolved) which would be due to the atomic dynamics. Second, the sidebands ($|W_{m+1}\rangle \leftrightarrow |W_{m-1}\rangle$) have a coupling strength which very rapidly decreases as U_0 increases (see fig. 11). In addition they are fully symmetric with respect to the carrier which results from eq. (16), and hence lead to no line pulling of the carrier. We have checked that the numerical calculations agree with this statement to within the accuracy of the calculations. This absence of shift and broadening remains true even for very shallow traps down to a depth of a few E_r , the ultimate limitation being the lifetime of the Wannier-Stark states. This situation is in striking contrast with the results of section III in the absence of gravity.

The system is more complex if the initial state of the atom is a coherent superposition of neighbouring wells.

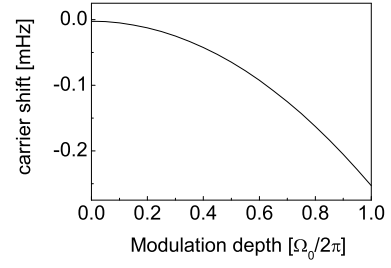


FIG. 13: Frequency shift of the carrier as a function of the square modulation depth (see caption of Fig. 12). The calculation has been performed for $U_0 = 5E_r$, $\Omega_0/2 = 10\text{ Hz}$ and an interaction time of $t_g/2 = 43.5$. The initial atomic state is the one corresponding to the dotted line in figure 12.

In this case off-resonant excitation of the sidebands will interfere with the carrier excitation with a relative phase which depends on the initial relative phase of neighbouring wells and on all the parameters of the atom-laser interaction (Δ_g , Ω_0 and the duration of the interaction). This interference leads to a modification of the carrier transition probability which is of the order of $\Omega_0/2 = \Omega_g$ (for the first, and most significant, sideband). For an interaction close to a π pulse, an order of magnitude of the corresponding carrier pulling is then $\Omega_0/2 = \Omega_g$ which can be significant. As an example for $U_0 = 10E_r$ and $\Omega_0/2 = 10\text{ Hz}$ the shift is about $2 \times 10^{-2}\text{ Hz}$, i.e. several times 10^{-17} of the clock transition frequency. This shift is a priori all the more problematic as the initial atomic state is difficult to know and control accurately.

We have numerically solved eq. (17) for various initial atomic states, lattice depths and interaction parameters to get a more quantitative insight of the effect. The results are illustrated in figure 12 for the case $U_0 = 5E_r$. A clear signature of the effect can be identified from its dependence on the interaction duration: the frequency shift oscillates with a frequency $\Omega_g/2$ resulting from the Ω_g term in Ω_m in (17). This provides a powerful method for investigating site-to-site coherences in the lattice. More interestingly from a clock point of view, the shift becomes negligible for all interaction durations t such that $t = (n+1/2)t_g$. For these interaction durations the interference from the sidebands is symmetric for positive and negative detunings from resonance, leading to no overall shift. Since Ω_g is extremely well known (potentially at the 10^{-9} level) this condition can be accurately met. Note that choosing such a value of the interaction duration does not significantly affect the contrast, as the two relevant timescales have different orders of magnitude in the narrow resonance limit ($\Omega_0 \gg \Omega_g$), and therefore a range of values of t such that $t = (n+1/2)t_g$ correspond to almost optimal contrast (e.g. all such values of t in figure 12). A more detailed study shows that the level of cancellation depends on the depth of the modulation used to determine the frequency shift (see caption of Fig. 12) which results from a slight distortion of the carrier resonance. This

effect is shown in figure 13, which clearly indicates that the shift can be controlled to below 1 mHz even for a very shallow lattice depth down to $U_0 = 5E_r$.

V. DISCUSSION AND CONCLUSION

We studied the trap depth requirement for the operation of an optical lattice clock with a projected fractional accuracy in the 10^{-17} – 10^{-18} range. We have shown that using a purely periodic potential necessitates a lattice of depth $50-100E_r$ limited by tunnelling between adjacent sites of the lattice. A possible way to vastly reduce this depth is to use gravity to lift the degeneracy between the potential wells which strongly inhibits tunnelling. Trap depths down to $5-10E_r$ are then sufficient to cancel the effects of the atom dynamics at the desired accuracy level. This will become even more important for future work aiming at even higher accuracies. Although very simple, gravity is not the only way to suppress tunnelling and other solutions, essentially consisting in a dynamic control of the lattice, are certainly possible [38, 39, 40]. They may prove useful if one wants to operate a lattice clock in space for instance.

Throughout the paper we have not taken into account the dynamics of the atoms in the directions transverse to the probe beam propagation. Experimental imperfections however (misalignment, wavefront curvature, aberrations) may lead to a residual sensitivity to this dynam-

ics. If for example the probe beam is misaligned with respect to the vertical lattice by 100 μ rad the transverse wavevector k_\perp is about $10^{-4} k_s$ and a modest transverse confinement should be sufficient to make its effect negligible. Such a confinement can be provided by the gaussian transverse shape of the laser forming the lattice or by a 3D lattice. The latter also leads to an interesting physical problem depending on the relative orientation of the lattice with respect to gravity [41].

Finally the well-defined energy separation between Wannier-Stark states and the possibility to drive transitions between them on the red or blue sideband of the spectrum (section IV B) opens new possibilities for the realization of atom interferometers. This provides a method to generate a coherent superposition of distant states for the accurate measurement of the energy separation between these states. This can for instance lead to an alternative determination of g or \hbar/m_a [42, 43, 44, 45].

ACKNOWLEDGEMENTS

We thank Sebastien Bize, Andre Clairon and A maud Landragin for fruitful and stimulating discussions, as well as Fosse Laurent for motivating this work. SYRTE is Unité Associée au CNRS (UMR 8630) and acknowledges support from Laboratoire National de Métrologie et d'Essai (LNE).

-
- [1] R. H. Dicke, Phys. Rev. 89, 472 (1953).
 - [2] N. Ramsey, Molecular beams (Oxford University Press, Oxford, 1985).
 - [3] P. H. Lee and M. L. Skolnick, Appl. Phys. Lett. 10, 303 (1967).
 - [4] F. Biraben, B. Cagnac, and G. Grynberg, Phys. Rev. Lett. 32, 643 (1974).
 - [5] D. Leibfried, R. Blatt, C. Monroe, and D. Wineland, Rev. Mod. Phys. 75, 281 (2003).
 - [6] C. Cohen-Tannoudji, S. Chu, and W. Phillips, Rev. Mod. Phys. 70, 685 (1998).
 - [7] D. Berkeland et al., Phys. Rev. Lett. 80, 2089 (1998).
 - [8] T. Udem et al., Phys. Rev. Lett. 86, 4996 (2001).
 - [9] J. Stenger et al., Opt. Lett. 26, 1589 (2001).
 - [10] A. A. Madej et al., Phys. Rev. A 70, 012507 (2004).
 - [11] H. S. Margolis et al., Science 306, 1355 (2004).
 - [12] B. Young, F. Cuzzo, W. Itano, and J. C. Bergquist, Phys. Rev. Lett. 82, 3799 (1999).
 - [13] A. Quesada et al., J. Opt. B : Quantum Semiclassical Opt. 5, S150 (2003).
 - [14] S. Bize et al., C. R. Physique 5, 829 (2004).
 - [15] P. Wolf and C. J. Borde, ArXiv:quant-ph/0403194.
 - [16] R. Li and K. Gibble, Metrologia 41, 376 (2004).
 - [17] C. J. Borde et al., Phys. Rev. A 30, 1836 (1984).
 - [18] J. Ishikawa, F. Riehle, J. Helmcke, and C. J. Borde, Phys. Rev. A 49, 4794 (1994).
 - [19] C. J. Borde, Metrologia 39, 435 (2002).
 - [20] U. Sterr et al., C. R. Physique 5, 845 (2004).
 - [21] C. W. Oates, G. W. Hilbers, and L. Hollberg, Phys. Rev. A 71, 023404 (2005).
 - [22] H. Katori, M. Takamoto, V. G. Palchikov, and V. D. Ovsiannikov, Phys. Rev. Lett. 91, 173005 (2003).
 - [23] I. Courtillot et al., Phys. Rev. A 68, R030501 (2003).
 - [24] T. Hong, C. Cramer, W. Nagourney, and E. N. Fortson, Phys. Rev. Lett. 94, 050801 (2005).
 - [25] R. Santra et al., ArXiv:physics/0411197 (2004).
 - [26] S. G. Porsev and A. Derevianko, Phys. Rev. A 69, 042506 (2004).
 - [27] G. Nenciu, Rev. Mod. Phys. 63, 91 (1991).
 - [28] M. Glück, A. Kolovsky, H. Korsch, and N. Moiseyev, Euro. Phys. J. D 4, 239 (1998).
 - [29] N. W. Ashcroft and N. D. Mermin, Solid State Physics (Saunders, Philadelphia, 1976).
 - [30] M. Takamoto and H. Katori, Phys. Rev. Lett. 91, 223001 (2003).
 - [31] C. Zener, Proc. R. Soc. London Ser. A 137, 696 (1932).
 - [32] L. Landau, Phys. Z. Sov. 1, 46 (1932).
 - [33] E. Peik et al., Phys. Rev. A 55, 2989 (1997).
 - [34] C. F. Bhanu et al., Phys. Rev. A 55, R857 (1997).
 - [35] G. H. Wannier, Phys. Rev. 117, 432 (1960).
 - [36] J. Callaway, Phys. Rev. 130, 549 (1963).
 - [37] J. Avron, Ann. Phys. 143, 33 (1982).
 - [38] F. Grossmann, T. Dittrich, P. Jung, and P. Hanggi, Phys. Rev. Lett. 67, 516 (1991).
 - [39] R. B. Diener et al., Phys. Rev. A 64, 033416 (2001).
 - [40] H. L. Harutyunyan and G. Nienhuis, Phys. Rev. A 64,

- 033424 (2001).
- [41] M. G. Luck, F. Keck, A. R. Kolovsky, and H. J. Korsch, *Phys. Rev. Lett.* **86**, 3116 (2001).
 - [42] D. S. Weiss, B.-C. Young, and S. Chu, *Appl. Phys. B* **59**, (1994).
 - [43] S. Gupta, K. Diekmann, Z. Hadzibabic, and D. E. Pritchard, *Phys. Rev. Lett.* **89**, 140401 (2002).
 - [44] R. Battesti et al, *Phys. Rev. Lett.* **92**, 253001 (2004).
 - [45] G. Modugno et al, *Fortschr. Phys.* **52**, 1173 (2004).
 - [46] M. G. Luck, A. Kolovsky, and H. J. Korsch, *Phys. Rev. Lett.* **83**, 891 (1999).
 - [47] note that this effect cannot be quantified without an accurate knowledge of the magic wavelength and of the strength of transitions involving highly excited states.
 - [48] See section V for a brief discussion of the 3D problem
 - [49] This exponential increase is true on average only and can be modified for specific values of U_0 by a resonant coupling between states in distant wells [34, 37, 46].
 - [50] For similar reasons as in section III one can neglect the coupling to excited bands in the system for narrow enough resonances.